Formulation of Envelope Correlation Coefficient for Multiple Sensors Based on Scattering Parameter

MOHD ADZIMNUDDIN MOHD NOR AZAMI, MOHAMAD ZOINOL ABIDIN ABD. AZIZ
Fakulti Teknologi dan Kejuruteraan Elektronik
dan Komputer
Universiti Teknikal Malaysia Melaka
Hang Tuah Jaya, 76100, Durian Tunggal, Melaka
MALAYSIA

Abstract: - The Envelope Correlation Coefficient (ECC) is crucial for assessing multiple sensor systems in wireless communication, sensing, and microwave imaging. ECC measures signal similarity between sensors, with higher values (close to 1.00) indicating strong correlation. Efficient power transmission, reception, and multiband path transmission enhance sensor network performance by improving data rates and reliability through multiple frequency bands. This study uses scattering parameters to calculate ECC for four different sensors in a single arrangement. Most of the sensors exhibit higher correlation at f2 and f3, while f1 shows a low ECC.

Key-Words: - Envelope Correlation Coefficient, Monopole Structure Sensors, Triband and Dual-band Sensors

Received: April 8, 2024. Revised: September 13, 2024. Accepted: October 3, 2024. Published: November 4, 2024.

1 Introduction

n MIMO communication systems, the correlation between signals received from different sensors is measured by the Envelope Correlation Coefficient (ECC), which significantly impacts system performance parameters, including diversity gain and capacity. Strong correlation is indicated by a high ECC (near 1.00), whereas signal independence is demonstrated by a low ECC (near 0.00) [1]. The use of ECC in microwave imaging for security screening, non-destructive testing, and medical diagnostics is understudied despite its extensive research in MIMO. High ECC can enhance the redundancy and coherence of signals, leading to better resolution and accuracy in imaging [2]. For sensor networks, especially in situations where direct electrical connections are impractical, efficient power transmission and reception are important. Consistent power is maintained using methods such as radiative power transmission, resonant inductive coupling, and inductive coupling. Moreover, the implementation of multiband path transmission further enhances sensor network performance. By utilizing multiple frequency bands, multiband transmission improves data rate and reliability, reduces interference, and maximizes bandwidth utilization. This capability is particularly beneficial in dynamic environments where sensor networks must adapt to varying conditions.

Appropriate analytical techniques are used to calculate ECC, which can be done using three methods. The first method, based on the far-field radiation pattern, is time-consuming and involves detailed numerical or experimental analysis [3-6]. This method makes it necessary to do appropriate numerical or experimental analysis, which makes it a time-consuming procedure. The second method uses Clarke's formula and has gained popularity recently [7-9]. The third method, used in this study, employs scattering parameters from the sensor's elements, making it suitable for experimental measurements [10-12]. In this study, the ECC of four pairs of sensors, using scattering parameters, was analyzed. The sensors have different resonant frequencies, ranging from dual-band to tri-band.

2 Formulation

The fundamental Equation (1) [3] that calculate the ECC requires 3-dimensional radiation pattern consideration.

$$\rho_e = \frac{\left|\iint_{4\pi}\left[\overrightarrow{F_1}(\theta,\phi)\bullet\overrightarrow{F_2}(\theta,\phi)\right]d\Omega\right|^2}{\iint_{4\pi}\left|\overrightarrow{F_1}(\theta,\phi)\right|^2 d\Omega \iint_{4\pi}\left|\overrightarrow{F_2}(\theta,\phi)\right|^2 d\Omega} \quad (1)$$

The parameter $\overrightarrow{F_1}(\theta, \phi)$ is the field radiation pattern of the sensors. This parameter can only be used when port i is excited, and all other ports are terminated to a 50 Ω load. The symbol of • denotes the Hermitian product, which is used in linear algebra and quantum mechanics.

On the other hand, ECC can also be defined using a closed-form equation that utilizes the scattering parameters of the sensors. For this study, Equation 2 [3] is suitable as a good approximation due to its uniform distribution. Scattering parameters for two-element sensors can be described as follows:

$$\rho_e = \frac{|S_{11} * S_{12} + S_{21} * S_{22}|^2}{(1 - |S_{11}|^2 - |S_{21}|^2)(1 - |S_{22}|^2 - |S_{12}|^2)} (2)$$

The radiation pattern in Equation (1) is much more complicates the calculations compared to the envelope correlation in Equation (2). The second equation is straightforward to use and produces accurate results in all situations, even inside with high multipath propagation performance.

3 Sensors Configuration

The mathematical formula in Equation 2 requires the scattering performance from two identical sensors. In this study, four pairs of sensors with transmitters and receivers operating at different frequencies have been used to study the ECC. Fig. 1 shows the printed four pairs of sensors. These sensor pairs are referred to as Sensor 1, Sensor 2, Sensor 3, and Sensor 4. The characteristics of these sensors are summarized in Table 1. Each transmitter and receiver pair has a similar resonant frequency. Fig. 2 shows the return loss of Sensors 1 through 4.

Sensor 1 has a triband operating frequency at 1.67, 2.15, and 2.64 GHz with return losses of 22.07, 24.34, and 20.50 dB, respectively. Sensors 2 through 4 have dual-band operating frequencies. Sensor 2 operates at 1.69 and 2.16 GHz with return losses of 20.31 and 21.47 dB, respectively. Sensor 3 has the lowest return loss, at 19.40 and 16.88 dB, with operating frequencies at 1.70 and 2.65 GHz. Lastly, Sensor 4 has resonant frequencies at 2.16 and 2.57 GHz with return losses of 21.26 and 11.24 dB, respectively. The vector network analyzer used is a portable vector network analyzer (NanoVNA V2).

The introduced sensor system has been studied and investigated in terms of ECC measurement using a circular arrangement. Pairs of Sensors 1 through 4 are connected using individual portable vector network analyzers, and scattering parameters are recorded, as shown in Fig. 3. The arrangement was set with Sensors 1 through 4 arranged in a circle, with a distance of 20 cm between each transmitter and receiver. The illustration of this arrangement is shown in Fig. 4. As depicted, the arrangement starts with the transmitter of Sensor 2 placed side by side with the transmitter of Sensor 4 and the receiver of Sensor 3. The transmitter of Sensor 1 is adjacent to the transmitters of Sensors 4 and 3. The measurement of ECC has been repeated 50 times for all configurations to ensure the data is consistent and reliable.

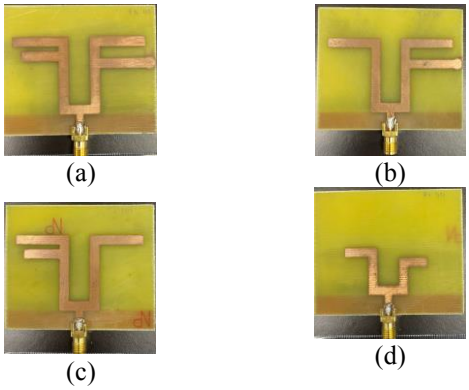

Fig.1 Fabricated Sensor (a) Sensor 1, (b) Sensor 2, (c) Sensor 3, (d) Sensor 4

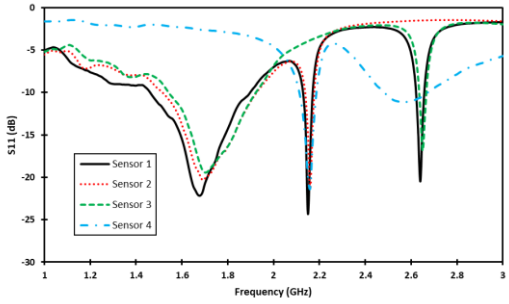

Fig. 2 Sensor's return loss

Table 1. Sensor's resonant frequencies

Sensor	Resonant Frequency (GHz)			Return Loss (-dB)		
	f1	f2	f3	f1	f2	f3
1	1.67	2.15	2.64	22.07	24.34	20.50
2	1.69	2.16		20.31	21.47	
3	1.70		2.65	19.40		16.88
4		2.16	2.57		21.26	11.24

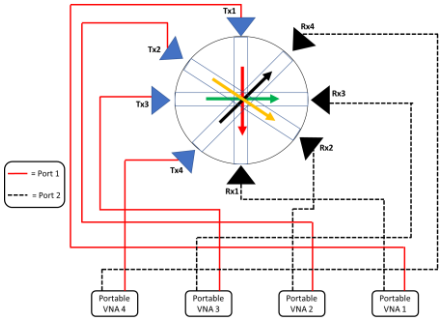

Fig.3 4x4 MIMO communication system setup

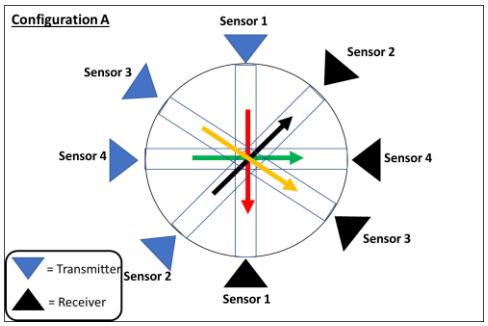

Fig.4 Sensor's arrangement

4 Result and Discussion

The arrangement of the sensors has been studied and investigated in terms of ECC measurements. The corresponding results have been obtained for each configuration and each sensor. To use the mathematical formula proposed by Equation (2), the corresponding S-parameters have been measured from all the sensors, as shown in Table 2. Table 2 presents the values of S11, S21, S12, and S22 for all sensors at each resonant frequency. The data is taken as the range between the maximum and minimum values of the S-parameters across 50 sets of data. For example, the highest value of S11 was recorded for Sensor 3 at f1, which is -23.00 dB. Using the data from Table 2, the ECC value can be calculated using the mathematical formula in Equation (2).

Table 2. The result of S-Parameter for all sensors

Config.	Sen.	Freq	S11		S21		S12		S22	
			Min	Max	Max	Min	Max	Min	Min	Max
A	1	f1	-15.37	-17.09	-28.03	-29.72	-28.31	-29.70	-15.38	-17.07
		f2	-10.03	-10.22	-24.46	-25.00	-24.52	-24.99	-10.02	-10.23
		f3	-3.80	-3.89	-30.34	-31.00	-30.81	-31.40	-3.82	-3.90
	2	f1	-14.49	-14.69	-24.51	-25.46	-24.50	-25.45	-14.50	-14.70
		f2	-10.03	-10.22	-24.46	-25.00	-24.52	-24.99	-10.02	-10.23
	3	f1	-20.68	-23.00	-31.78	-34.92	-31.88	-34.91	-20.72	-22.93
		f3	-5.26	-5.52	-40.01	-41.01	-40.10	-41.06	-5.26	-5.52
	4	f2	-10.78	-11.11	-23.50	-23.74	-23.48	-23.74	-10.79	-11.13
		f3	-6.97	-7.77	-20.72	-22.31	-20.85	-21.35	-7.29	-7.53

Fig. 5 presents the ECC values for Sensors 1 to 4 across frequencies f1 to f3. From the figure, it is evident that f1 shows the lowest ECC among all frequencies for all sensors. Sensor 2 has an ECC value of 0.61, while Sensor 3 has the lowest ECC value of 0.15. Meanwhile, at f2 and f3, most sensors exhibit ECC values closer to 1.00, indicating better signal correlation. At f1, the lower ECC values suggest that the propagation environment might be causing more multipath interference, leading to less coherent signal reception across the sensors. Multipath interference occurs when signals take different paths to reach the sensor, causing them to arrive at different times and phases. Conversely, the higher ECC values at f2 and f3 suggest that the signals travel better and face less interference at these frequencies. As a result, the signals are more stable and experience less disruption, leading to stronger and more consistent readings from the sensors.

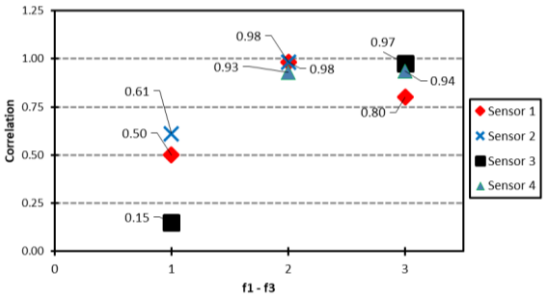

Fig.5 Value of ECC for Sensor 1 – Sensor 4

5 Conclusion

The analysis of ECC values across different frequencies has been conducted in this experiment. The low ECC values at f1 indicate a challenging propagation environment with higher multipath interference and signal degradation, leading to weaker correlation between the sensors. Conversely, the higher ECC values at f2 and f3 suggest a more favorable propagation environment with reduced interference and more stable signal paths, enhancing signal coherence and correlation.

Acknowledgment

This work was supported by the Universiti Teknikal Malaysia Melaka under the FRGS research grant (FRGS/1/2021/FKEKK/F00471), and by the Ministry of Higher Education of Malaysia.

References:

[1] P. Sharma, R. N. Tiwari, P. Singh, P. Kumar, and B. K. Kanaujia, "MIMO Antennas: Design Approaches, Techniques and Applications," *Sensors (Basel, Switzerland)*, vol. 22, no. 20. NLM (Medline), Oct. 14, 2022. doi: 10.3390/s22207813.

[2] S. H. Kiani, H. S. Savci, M. E. Munir, A. Sedik, and H. Mostafa, "An Ultra-Wide Band MIMO Antenna System with Enhanced Isolation for Microwave Imaging Applications," *Micromachines (Basel)*, vol. 14, no. 9, Sep. 2023, doi: 10.3390/mi14091732.

[3] C. Votis, G. Tatsis, and P. Kostarakis, "Envelope Correlation Parameter Measurements in a MIMO Antenna Array Configuration," *International Journal of Communications, Network and System Sciences*, vol. 03, no. 04, pp. 350–354, 2010, doi: 10.4236/ijcns.2010.34044.

[4] N. Honma and K. Murata, "Correlation in MIMO antennas," *Electronics (Switzerland)*, vol. 9, no. 4, Apr. 2020, doi: 10.3390/electronics9040651.

[5] E. Fritz Andrade *et al.*, "Discrete formulation of envelope correlation coefficient for faster analysis in MIMO antenna systems," *Ingeniería Investigación y Tecnología*, vol. 23, no. 4, pp. 1–14, Jul. 2022, doi: 10.22201/fi.25940732e.2022.23.4.028.

[6] D. Sarkar, S. Mikki, K. V. Srivastava, and Y. Antar, "Far-field Envelope Correlation Coefficient and Near-field Reactive Energy of MIMO Antennas: An FDTD-IDM-CGF Approach."

[7] C. Christodoulou, T. W. C Brown, and U. M. Ekpe, "Wireless Corner Eva Rajo-Iglesias When is Clarke's Approximation Valid?"

[8] Y. Karasawa and H. Iwai, "Transactions Letters Modeling of Signal Envelope Correlation of Line-of-Sight Fading with Applications to Frequency Correlation Analysis," 1994.

[9] Institute of Electrical and Electronics Engineers and EurAAP., *2017 11th European Conference on Antennas and Propagation (EuCAP) : 19-24 March 2017.*

[10] Y. A. S. Dama *et al.*, "An envelope correlation formula for (N, N) MIMO antenna arrays using input scattering parameters, and including power losses," *Int J Antennas Propag*, vol. 2011, 2011, doi: 10.1155/2011/421691.

[11] S. Wang, "Envelope Correlation Coefficient for Logarithmic Diversity Receivers Revisited," *IEEE Transactions on Communications*, vol. 55, no. 11, pp. 2042–2046, 2007, doi: 10.1109/TCOMM.2007.908507.

[12] J. Thaysen and K. B. Jakobsen, "Envelope correlation in (N, N) mimo antenna array from scattering parameters," *Microw Opt Technol Lett*, vol. 48, no. 5, pp. 832–834, May 2006, doi: 10.1002/mop.21490.

Contribution of Individual Authors to the Creation of a Scientific Article (Ghostwriting Policy)

The authors equally contributed in the present research, at all stages from the formulation of the problem to the final findings and solution.

Sources of Funding for Research Presented in a Scientific Article or Scientific Article Itself

No funding was received for conducting this study.

Conflict of Interest

The authors have no conflicts of interest to declare that are relevant to the content of this article.